Computers & Geosciences 42 (2012) 79–86

Contents lists available at SciVerse ScienceDirect

Computers & Geosciences

journal homepage: www.elsevier.com/locate/cageo

Estimating future global per capita water availability based on changes in climate and population

Esther S. Parish [a], Evan Kodra [b], Karsten Steinhaeuser [c], Auroop R. Ganguly [b,*]

[a] Environmental Sciences Division, Oak Ridge National Laboratory (ORNL), Oak Ridge, TN 37831, USA
[b] Civil and Environmental Engineering Department, Northeastern University, Boston, MA 02115, USA
[c] Department of Computer Science and Engineering, University of Minnesota, Minneapolis, MN 55455, USA

ARTICLE INFO

Article history:
Received 22 September 2011
Received in revised form
16 December 2011
Accepted 26 January 2012
Available online 18 February 2012

Keywords:
Climate change impacts
Population growth
Resource scarcity
Water availability

ABSTRACT

Human populations are profoundly affected by water stress, or the lack of sufficient per capita available freshwater. Water stress can result from overuse of available freshwater resources or from a reduction in the amount of available water due to decreases in rainfall and stored water supplies. Analyzing the interrelationship between human populations and water availability is complicated by the uncertainties associated with climate change projections and population projections. We present a simple methodology developed to integrate disparate climate and population data sources and develop first-order per capita water availability projections at the global scale. Simulations from the coupled land–ocean–atmosphere Community Climate System Model version 3 (CCSM3) forced with a range of hypothetical greenhouse gas emissions scenarios are used to project grid-based changes in precipitation minus evapotranspiration as proxies for changes in runoff, or fresh water supply. Population growth changes, according to Intergovernmental Panel on Climate Change (IPCC) storylines, are used as proxies for changes in fresh water demand by 2025, 2050 and 2100. These freshwater supply and demand projections are then combined to yield estimates of per capita water availability aggregated by watershed and political unit. Results suggest that important insights might be extracted from the use of the process developed here, notably including the identification of the globe's most vulnerable regions in need of more detailed analysis and the relative importance of population growth versus climate change in altering future freshwater supplies. However, these are only exemplary insights and, as such, could be considered hypotheses that should be rigorously tested with multiple climate models, multiple observational climate datasets, and more comprehensive population change storylines.

1. Introduction

One recent work has concluded that almost 80% of the world's population is exposed to significant fresh water security threats via multiple stressors (Vörösmarty et al., 2010), two of which are population and climate change. Water stress can be qualitatively defined as the lack of sufficient fresh water for domestic, agricultural, and/or industrial needs. Water stress may result from overuse of water supplies due to population increase, industrialization, and/or lack of conservation practices, as well as from decreased rainfall due to changes in climate and/or lack of storage capacity in areas that receive variable amounts of water throughout the year. Building on work by Falkenmark (e.g., Falkenmark, 1986), world relief agencies commonly define conditions of "water stress" as less than 1700 m^3 of available water per person per year and "severe water stress" as less than 1000 m^3 per person per year; we also adopt those definitions for this work. This widely accepted method of estimating "water stress" is based on the fact that lack of freshwater availability imposes constraints on food production and industrial development that tend to scale with population growth (Edwards et al., 2005). A 2003 study by the World Resources Institute (WRI, 2003) concluded that 48 percent of the world's projected population (~3.5 billion people) will live in water-stressed river basins by 2025. According to the World Meteorological Organization (Shiklomanov, 1997), water availability will be one of the major challenges facing human society in the 21st century, and lack of water will be one of the key factors limiting development in many areas of the world. Determination of future water availability is further complicated by water quality, which may be adversely affected by competition resulting from increases in population (Vörösmarty et al., 2000) as well as consequences of climate change such as sea level rise (Kundzewicz et al., 2008).

Analyzing the complex interrelationship between growing human populations and available water supplies is complicated

* Corresponding author. Tel.: +1 617 373 3710.
E-mail address: a.ganguly@neu.edu (A.R. Ganguly).

0098-3004/$ - see front matter © 2012 Elsevier Ltd. All rights reserved.
doi:10.1016/j.cageo.2012.01.019

by climate change projections and non-stationarity, or the traditional water-resource engineering concept that the hydrologic system fluctuates within an unchanging, manageable envelope of variability. Water stress is anticipated to combine with other stressors to exacerbate problems in areas already prone to regional instability, as indicated in recent publications such as the United Kingdom's Ministry of Defense Publication (DCDC, 2007).

Several studies quantified future water availability and pinpointed areas of potential water scarcity prior to the conception of the Intergovernmental Panel on Climate Change (IPCC) "storylines" of carbon emissions and population change (IPCC, 2007). A landmark study by Vörösmarty et al. (2000) derived global projections of water availability in 2025 compared to 1985 and concluded that changes in population and economic development will cause more changes in water stress than changes in climate. Alcamo and Henrichs (2002) compared global projected water availability in 2032 to a baseline scenario of 1995 using the WaterGAP model to relate changes in national income to changes in water use per person and per unit of generated electricity under four different social/economic scenarios. They calculated water stress as the average annual withdrawals-to-availability ratio 0.4 or greater and found that severe water stress would be most likely in parts of central Mexico, the Middle East, large parts of the Indian sub-continent, and stretches of the North African coast (Alcamo and Henrichs, 2002). An exemplary analysis following the definition of Falkenmark (1986) (see introduction) is contained in the 2003 WRI "Water Resources eAtlas" produced by WRI, the International Water Management Institute (IWMI)'s "Watersheds of the World Map 15," showing the annual renewable water supply (m^3/person/year) per major basin for 1995 and for 2025 based upon 1995 census data, UN lower-end projections for population growth (such that global population peaks at 7.2 billion in 2025), and global runoff results developed by the University of New Hampshire and the WMO/Global Runoff Data Center. This 2003 WRI study concluded that 48% of the world's population will live in water-stressed river basins by 2025.

Following the development of the 2000 IPCC SRES socioeconomic storylines, Arnell (2004) used 30-year-mean climate projections from six global climate models (GCMs) in conjunction with the Gridded Population of the World (GPW) version 2 datset (Deichmann et al., 2001) to evaluate potential areas of water stress in terms of Falkenmark's water scarcity index. Arnell (2004) found that the Mediterranean, parts of Europe, the central and southern United States, and southern Africa will most likely experience increased water stress as a consequence of climate change.

In this work, we develop a data integration, analysis, and visualization process to estimate future per capita freshwater water availability and potential areas of water stress across the globe using updated global climate change projections and concurrent population change projections. We have developed this toolkit using the Oak Ridge National Laboratory's state-of-the-art high-resolution gridded population dataset, Global LandScan (Dobson et al., 2000) in conjunction with the regionally disaggregated IPCC (2007) socioeconomic storylines. We have derived our freshwater availability from a fully integrated earth system model, the Community Climate System Model, version 3 (CCSM3) (e.g., Drake et al., 2005), where the disadvantages of lower resolution are balanced by the ability to consider the land-atmosphere feedback effects. The methodology and toolkit that we have developed is flexible enough to enable incorporation of other population and climate projections as they become available.

Exemplary use cases of this tool that are explored here include: (1) determine potential human impacts at global and regional scales; (2) determine if there might be any new "hot spots" of water scarcity under a changing climate regime that might require higher resolution analyses for planning and mitigation purposes; and (3) assess the relative (proportional) roles of global and regional population versus climate change as drivers of water availability, thus ultimately informing where adaptation and/or mitigation efforts ought to be directed. Section 2 details the choices of data and methodology, including a brief discussion on population and climate change uncertainty as it relates to these choices; Section 3 details exemplary results from the analysis; Section 4 summarizes the objectives and significance of this work and suggests possible future direction for this line of research.

2. Data and methodology

Previous studies of global water resources (Section 1) have fed climate outputs from GCMs into higher-resolution hydrology models to estimate renewable freshwater supplies (Alcamo and Henrichs, 2002; Alcamo et al., 2007; Arnell, 2004; Vörösmarty et al., 2000). While hydrological modeling is the state-of-the-art in this respect, it may also be of interest to estimate freshwater supplies directly from GCMs, thus preserving important fully-coupled interactions between atmosphere, ocean, land and sea-ice. Hence, one fully-coupled GCM which preserves these interactions, CCSM3, is used to demonstrate the data-integrative toolkit developed in this study. CCSM3 enables the approximation of changes in runoff, or available fresh water, via the calculation of precipitation minus evapotranspiration (P − E).

To position this paper in the context of prior art or the state of practice and to appropriately caveat our geographical assessments of water stress that follow, two considerations need further clarification: (a) uncertainty characterization for changes in climate and population, as they may be relevant for this study and (b) precision in the outputs based on the statistical or dynamical downscaling as well as water availability assessments based on models of surface water hydrology. Previous studies (e.g., Schneider and Kuntz-Duriseti, 2002: discussion on cascades of uncertainty) have suggested that uncertainties in the impacted human or built systems (population in this case) may dominate over uncertainties in natural systems (climate in this case). This paper does not attempt to account for uncertainties in population storylines or in their variability over space and time, which in turn may dominate for overall uncertainty assessments in the water stress computations. Neither does this work attempt to account for uncertainties in climate projections, which may be hypothesized to be smaller than the population uncertainties but would nevertheless, be important to consider. Uncertainty quantification using multiple climate models (i.e., model ensembles) is a complex subject in and of itself, especially since climate is a non-stationary system and model predictions are over long lead times ranging from multi-decadal to century scales. Significantly different perspectives on the appropriateness (e.g., Stainforth et al., 2007; Knutti et al., 2010; Knutti, 2010; Perkins et al., 2009) of and several approaches (e.g., Tebaldi et al., 2004; Greene et al., 2006; Pierce et al., 2009; Santer et al., 2009; Smith et al., 2009) for model ensemble prediction and uncertainty characterization can be found in the literature, which are problems that have yet to be solved. In our prior research, we have used both multi-model ensembles (e.g., Kodra et al., 2011, Kao and Ganguly, 2011) as well as a single-model (e.g., Ganguly et al., 2009) depending on the nature of the desired insights. A related issue is the development of precise projections based on statistical or dynamical (based on regional climate models) downscaling followed by their use in physically-based hydrological models. While this is another relevant, important research area, there is a need for caution because of the cascade of uncertainty among models (e.g., Scheirmeier, 2010, Schneider and Kuntz-Duriseto,

2002) and also because of the potential lack of feedback among serially-connected models.

The purpose of this discussion is to caveat our results and insights in light of the complexity of relevant uncertainties. A careful and rigorous treatment of uncertainty is left as future work for the purposes of this paper. Meanwhile, our results and geographical insights need to be viewed as representing plausible, exemplary scenarios of water stress, which are based on physically consistent projections of climate and socio-economically justifiable storylines of population.

2.1. Data

Storylines of 21st century changes in population and scenarios of per capita fossil fuel dependence were used in the development of IPCC SRES guidelines (IPCC, 2000) that dictate the greenhouse gas (GHG) trajectories, which force the global climate model CCSM3. To represent first-order changes in freshwater availability, decadal averages of P − E are obtained for the "current" time frame (2000–2009), for 2025 (2020–2029), for 2050 (2045–2054), and for 2100 (2090–2099); these variables were retrieved from one ensemble of CCSM3 run with the IPCC SRES fossil fuel emissions scenarios A1FI, A2, A1B and B1.All CCSM3 variables are currently (as of the writing of this manuscript) available via the Earth System Grid (http://www.earthsystemgrid.org/).

The IPCC SRES emissions scenarios were selected to span the range from low to high cumulative emissions projections. The A1FI scenario is the most fossil-fuel intensive scenario that results in total cumulative carbon dioxide emissions of more than 1800 gigatons (GtC) by 2100. The emissions, and hence the global-average temperature trajectory, from A1FI trends higher than all other IPCC SRES scenarios after 2030 and is considered the "worst case" IPCC SRES scenario. However, recent observations have shown that current emissions have been trending slightly higher than the A1FI illustrative marker scenario trendline (Le Quéré et al., 2009; Raupach et al., 2007). The A2 scenario results in "medium-high" cumulative total GHG emissions of 1450–1800 GtC by 2100, the A1B scenario results in "medium-low" total GHG emissions of 1100–1450 GtC by 2100, and the B1 scenario results in "low" total GHG emissions of less than 1100 GtC by 2100.

We adopt the definitions of water stress used by Falkenmark (1986) (see Section 1). Use of this indicator requires the use of human population data, and we use the freely available Global LandScan population distribution dataset (version 2007) prepared by the Oak Ridge National Laboratory as a proxy for "current" water demand (Dobson et al., 2000; Sabesan et al., 2007). LandScan is prepared as a 30 arc-second grid of current population distribution based upon disaggregated province-level census counts, proximity to roads, slope, land cover, and other features. Downscaled population change projections were obtained from Columbia University's CIESIN (2002) down-scaled country-level population projections for the moderate (identical) A1 and B1 population growth scenarios, where global population peaks at ~9 billion in 2050 and gradually declines for the rest of the century (note that these identical population numbers were used to formulate SRES emissions scenarios A1FI, A1B, and B1) and the largest population growth scenario, A2, where global population continuously increases for the entire 21st century (used to formulate emissions scenario SRES A2). Maps showing the country-level differences in these population growth scenarios in 2025, 2050 and 2100 (all relative to 2000) are shown in Fig. 1. Change ratios were derived from these estimates and applied to the static LandScan grid to get projected population distributions in 2025, 2050 and 2100 under the A1/B1 and A2 population

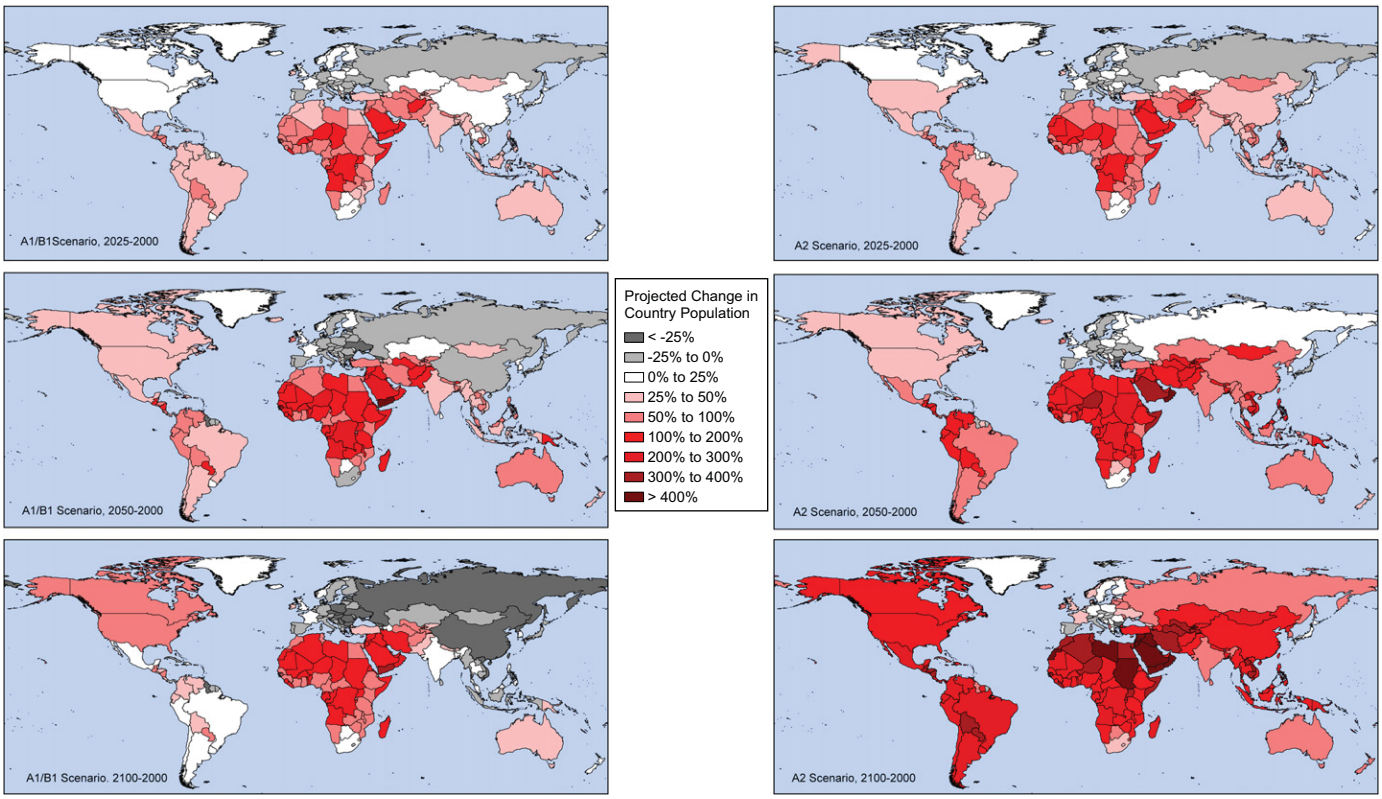

Fig. 1. Comparison of IPCC population storylines. IPCC SRES-projected changes in population are calculated using CIESIN downscaled country-level estimates. All panels display the change, in percentage, for years 2025, 2050, and 2100 relative to the year 2000. A constant rate of change is assumed for each country based on the IPCC storylines. Storyline A2 clearly diverges from A1/B1 by 2050, especially in the eastern hemisphere.

growth scenarios. These population changes were used as proxies for changes in water demand. Although the assumptions that population growth will be constant within countries and that per capita water usage will be the same in the future are oversimplified, we argue that this methodology is appropriate for a first-order analysis of global water availability intended to pinpoint regions most requiring future detailed studies.

Since available water (approximated in this study by P−E) is accumulated within watersheds, we aggregated the runoff volumes and population data by 26,929 global watersheds (see Section 4) and calculated the water stress index (m^3/person/year) for the range of low to high emissions scenarios (B1, A1B, A2 and A1FI) and four different time periods (baseline, 2025, 2050, and 2100).

2.2. Methodology

Freshwater accumulates within watersheds, or drainage basins, rather than political units. In order to analyze future freshwater availability, we first put together a layer of global watersheds based on two different datasets: the most detailed United States Geological Survey HYDRO1K basins available (Verdin and Greenlee, 1996) supplemented with Australian basins obtained from the Australian government's GIS data website (https://www.ga.gov.au). Together, these datasets yielded a total of 26,929 global watersheds with an average area of 5000 km^2.

We then calculated the amount of fresh water that would be available within each global basin at each time period under each scenario as follows: since CCSM3 is a fully-coupled GCM that captures interactions between the atmosphere, ocean, land and sea-ice, we approximated changes in runoff via the calculation of P−E. (Thus, contributions from groundwater and inter-basin transfers were not considered in this first-order analysis.) Total precipitation, or 'P', was calculated from the CCSM3 variables "RAIN+SNOW." Total evapotranspiration, or 'E', was calculated from the CCSM3 variables "QSOIL+QVEGE+QVEGT", a combination of ground evaporation, evaporation of canopy-intercepted water and canopy transpiration, respectively. The resulting P−E in mm/year is equivalent to "available precipitation" (Roy et al., 2010) or "internally renewable water resources" (FAO, 2003). Decadal averages of annual P−E at each grid cell were calculated with open-source statistical software R. These climate data were then imported into ArcGIS as points based upon latitude and longitude and spatially joined to a "fishnet" of polygons created using the same number of rows and columns as the T85 grid (where each grid cell is size 1.04625° × 1.04625°, and there are 256 (longitude) × 128 (latitude) grids). The resulting rectilinear

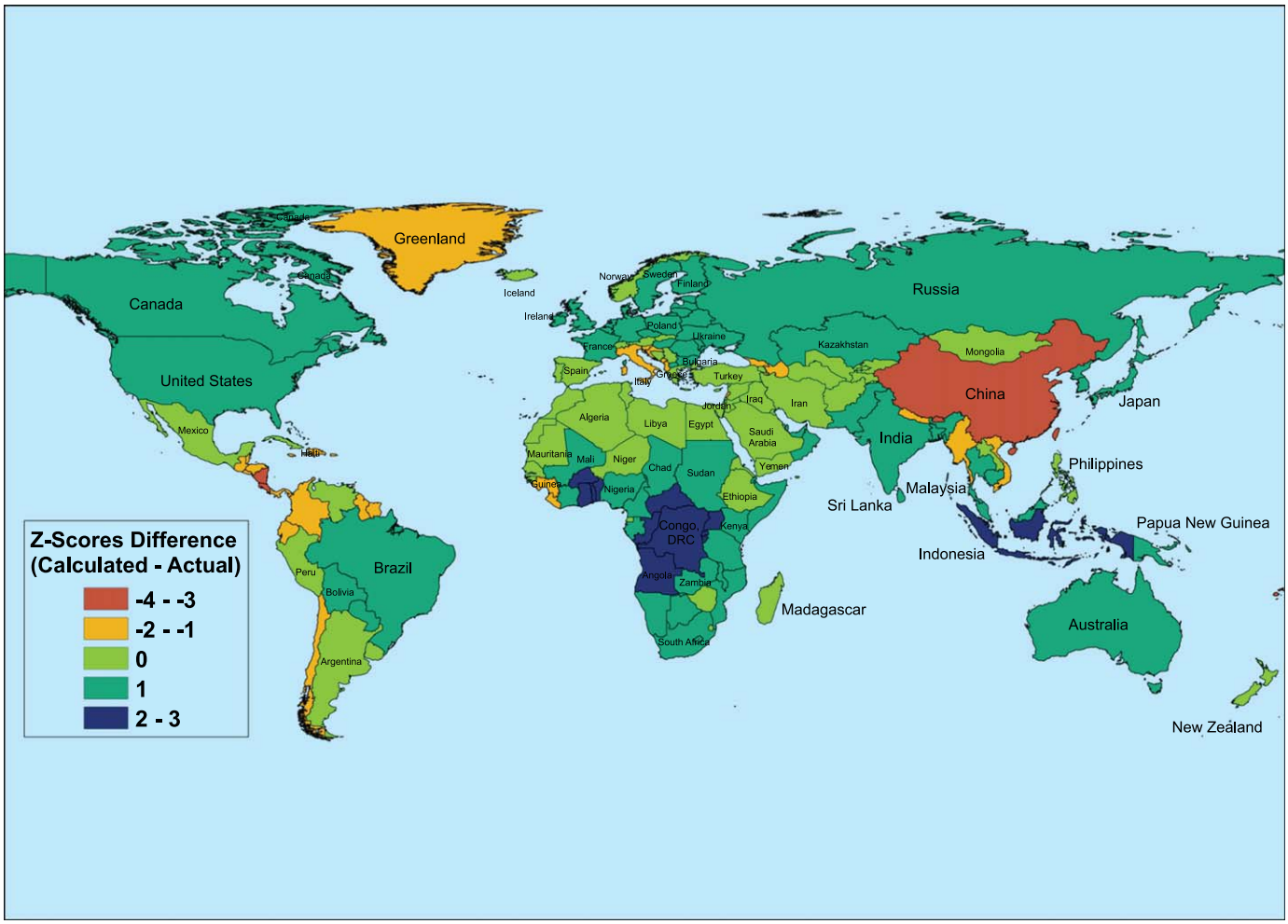

Fig. 2. Testing the skill of CCSM3-based calculations of freshwater availability using *Z*-scores. Rounded values of $Z_{c,diff}$ are calculated (Section 4) to compare 2000–2009 (decadally averaged) CCSM3 A1FI ("calculated") water availability aggregated by country to actual 2000–2009 (decadally averaged) water availability data by country collected by the UN FAO Aquastat program ("actual"). Areas shown in blue (brown) are over- (under)-estimated by the methodology. (For interpretation of the references to color in this figure legend, the reader is referred to the web version of this article).

climate polygons were then intersected with our layer of global watershed polygons described above. The area (in square meters) of each intersected portion was calculated. These intersected portions were then multiplied by the associated P−E values (converted from mm/yr to m/yr) and summed by basin in order to get an estimate of the total available water for each watershed in m^3/year at each time period (baseline, 2025, 2050 and 2100) under each emissions scenario (B1, A1B, A2 and A1FI).

The number of people living within a basin provides a first-order estimate of water demand since the amount of water that will be needed for agriculture and industry tends to be correlated to the total population. Future population was approximated for each basin using the following approach: ORNL's Global LandScan 2007 product described in Section 2.1 was used to represent baseline population for 2000–2009. CIESIN's downscaled country-level population growth ratios for 2025, 2050 and 2100 were applied to the static LandScan population grid in order to prepare estimates of population densities under each scenario at each time period. Some data preprocessing was required since the CIESIN dataset contains fewer countries than the Global LandScan dataset (e.g., 184 countries in CIESIN's table vs. 256 countries in the 2007 LandScan dataset); notably, Greenland and many of the smaller island nations are not included in the CIESIN file. Since many of the countries present in both datasets were named slightly differently, the nomenclature had to be standardized prior to comparison. Where there was no CIESIN projection for a particular country, we chose to use the existing population for all future years (i.e., conservatively assumed a static population in these areas). After preprocessing the current population data, we adjusted the "current" LandScan population (pop) numbers using the CIESIN A1/B1 and A2 growth ratios for each country according to the following formula:

$$\text{A1B1 Pop2025} = \text{LSPop2007} + (\text{CIESIN ratio for A1B1 pop in 2025 versus2005} * \text{LSPop2007})$$

For example, since CIESIN projected that the United States would have a population of 292,154,092 in 2005 and 348,577,770 in 2025 according the IPCC's A2 scenario, a growth rate of 19% percent was applied to each US grid cell from the Global LandScan dataset in order to obtain the projected 2025 A2 population distribution for the US. Where resulting population numbers were negative, we set the grid cells to 0. In this way, we prepared a series of eight current and projected population grids to cover the range of years and scenarios of interest (4 emissions scenarios for each of 2 population storylines).

In the final step, per capita water availability was calculated by dividing the estimated amount of runoff for each basin under each time period and emissions scenario by the number of people projected to be living in each basin under the corresponding time period and scenario. Based on these calculations of cubic meters/person/year, it could then be ascertained when and where water stress might occur.

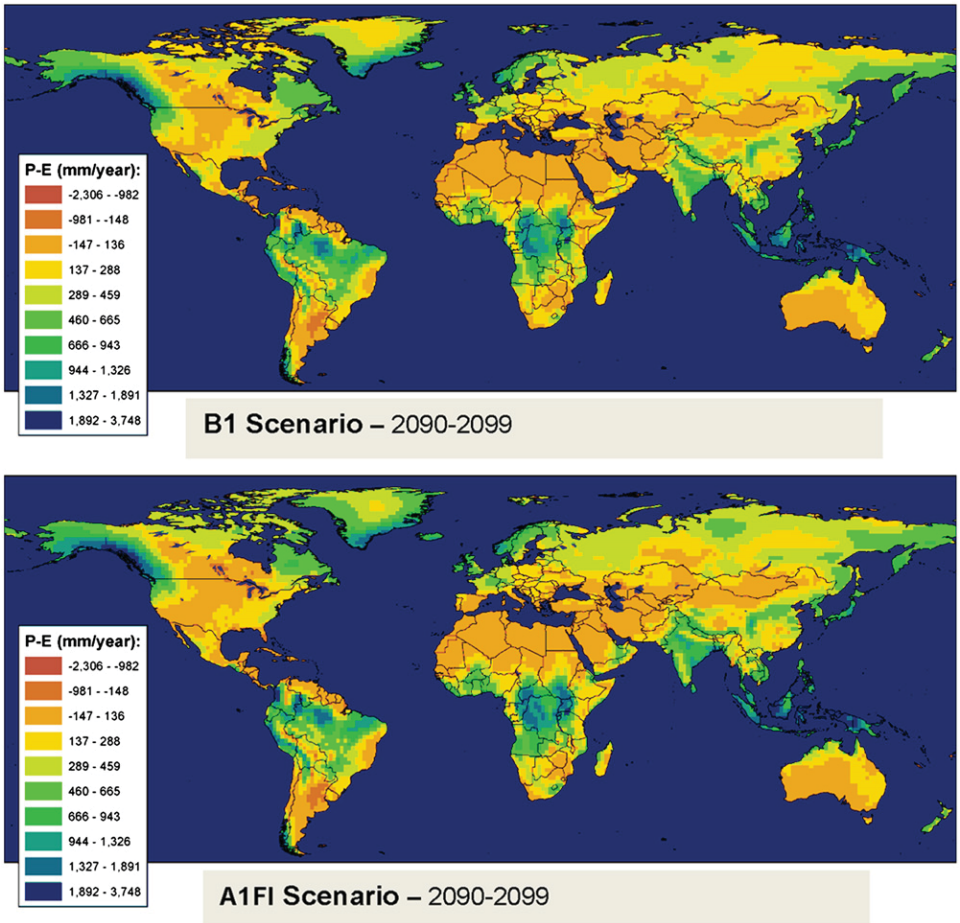

Fig. 3. P−E projections from CCSM3 for emissions scenario B1 and A1FI. CCSM3 runs for emissions scenarios B1 and A1FI (both using population storyline A1/B1) suggest that P−E (difference from 2000–2009 to 2090–2099) may change in many regions. However, it is not clear that emissions scenario seems to make a significant difference in the nature of the change; both maps here appear quite similar. This could suggest that emissions trajectories may not play as significant a role in dictating changes in P−E as will shifts in population.

2.3. Verification

A *Z*-score analysis was conducted as a first order method to evaluate the country-level accuracy of using CCSM3-based calculations of P−E to approximate freshwater availability. First, the methodology described in Section 2.2 was modified to calculate current runoff by country (rather than by drainage basin) in order to enable comparison to "actual" Food and Agricultural Organization (FAO, 2003) country-level estimates of internally renewable water resources (IRWR), defined as average annual flow of rivers and recharge of aquifers generated from endogenous precipitation, for the year 2000. After matching country names between datasets to the extent possible, *Z*-scores were generated for both actuals and CCSM3 data as $Z_c = (X_c - \mu)/\sigma$, where μ and σ are the average and standard deviation, respectively, of water availability (total cm/year averaged over 2000–2009) of all considered countries, X_c corresponds to the water availability of country c, and Z_c is the *Z*-score for country c. Differences in *Z*-scores from actuals and CCSM3 data are subsequently calculated ($Z_{c,diff} = Z_{c,CCSM3} - Z_{c,SASI}$). Larger $|Z_{c,diff}|$ values may suggest less accuracy. A resulting map of *Z*-score differences in calculated versus actual runoff (Fig. 2) suggests that our methodology significantly over-estimated water availability in central Africa and Indonesia and significantly under-estimated water availability in Central America and China.

3. Results

Calculations of projected per capita water availability are prepared based upon runoff results from one CCSM3 run with four emissions scenarios (B1, A1B, A2, and A1FI) with their respective population storylines (A1/B1, A1/B1, A2, A1/B1, respectively). Fig. 3 shows two exemplary maps of P−E, one for the lower-end emissions scenario B1 and one for the "Worst Case Emissions" scenario A1FI. Results suggest that P−E, or water availability, may change significantly in many regions in the 21st century. For example, western Canada and the lower hemispheric tropics may become substantially wetter, while in northern Africa, much of Asia, Australia, North America, and southern South America, CCSM3 projects drying. However, despite the vastly different emissions trajectories, at a global and continental scale, results from B1 and A1FI appear quite similar. On the other hand, the evolution of the two population storylines (A1/B1 and A2) displayed in Fig. 1, when considered alongside Fig. 3, would suggest that future per capita water availability may be more a function of population change than climate change.

This hints at an insight that becomes clearer with Fig. 4, which displays a graph summarizing the potential impacts to global basins and human population under each emissions scenario as the century progresses. The results here show A2 as the standout scenario, projecting far more water stress than any other. These results suggest that a population roughly equivalent to today's entire global population may experience water stress by the end of the century.

Next, we present exemplary results directly relevant to humans similar to Fig. 4 but at a regional scale. The graph in Fig. 5 summarizes water stress results for the continental United States, again suggesting that water demand from an increasing population may outpace changes in freshwater availability resulting from climate change. However, climate change still seems to be an extra stressor (e.g., an additional ~25 million people are projected to fall in the category of *very severe water stress* when moving from solely worst-case population change (under the A2 storyline) to the worst-case emissions increases (under the A1FI scenario) in combination with worst-case population change. This would suggest that freshwater availability changes resulting from global climate change should not be overlooked.

Also of interest may be the early identification of "hotspots", or regions that have an adequate fresh water supply now but may, via population and/or climate change, become vulnerable over the

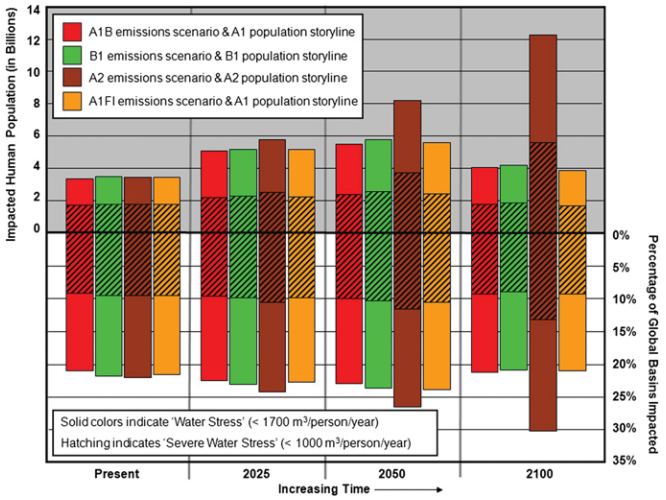

Fig. 4. Global projected water stress (based on per capita water availability). A range of IPCC SRES emissions scenarios and their accompanying population storylines are utilized to calculate multiple projected global water stress calculations. These results indicate that there will be at least a slight increase in the number of global basins and people impacted by water stress by the middle and latter part of the century. The largest increase in stress is likely to occur under the medium-high A2 emissions scenario, but further analysis has shown that this results more from the dramatically increasing global population under the A2 storyline rather than from increasing emissions. Under the A1/B1 population storyline, the population of most countries will decrease after 2050, thereby accounting for the decrease in water stress levels between 2050 and 2100 for the corresponding A1B, B1, and A1FI emissions scenarios.

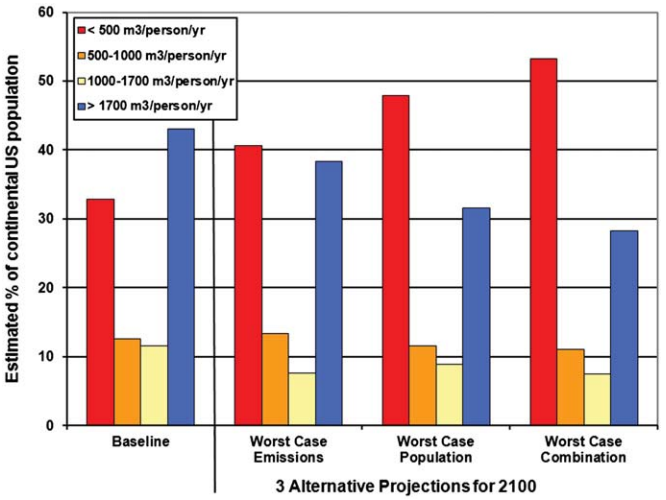

Fig. 5. Comparison of potentially water stressed continental United States population. A comparison of century-end per capita water availability projections for the continental US as compared to baseline conditions. The "Worst Case Emissions" scenario uses existing continental US population in combination with projected freshwater runoff under the highest (A1FI) emissions scenario. The "Worst Case Population" scenario uses current freshwater availability in combination with the population growth projected under the "worst-case" A2 population storyline. The "Worst case combination" scenario uses freshwater availability based on the highest emissions scenario (A1FI) in combination with the demand of the highest population scenario (A2) to project water stress in 2100. While the A1FI emissions scenario is technically based on the storyline of A1/B1 population growth, it is worth exploring different paths along which emissions could reach A1FI levels by the end of the 21st century; especially since population storylines and emissions scenarios are not exhaustive. This graph indicates that population may be the most influential determinant of future water stress within the continental US by 2100.

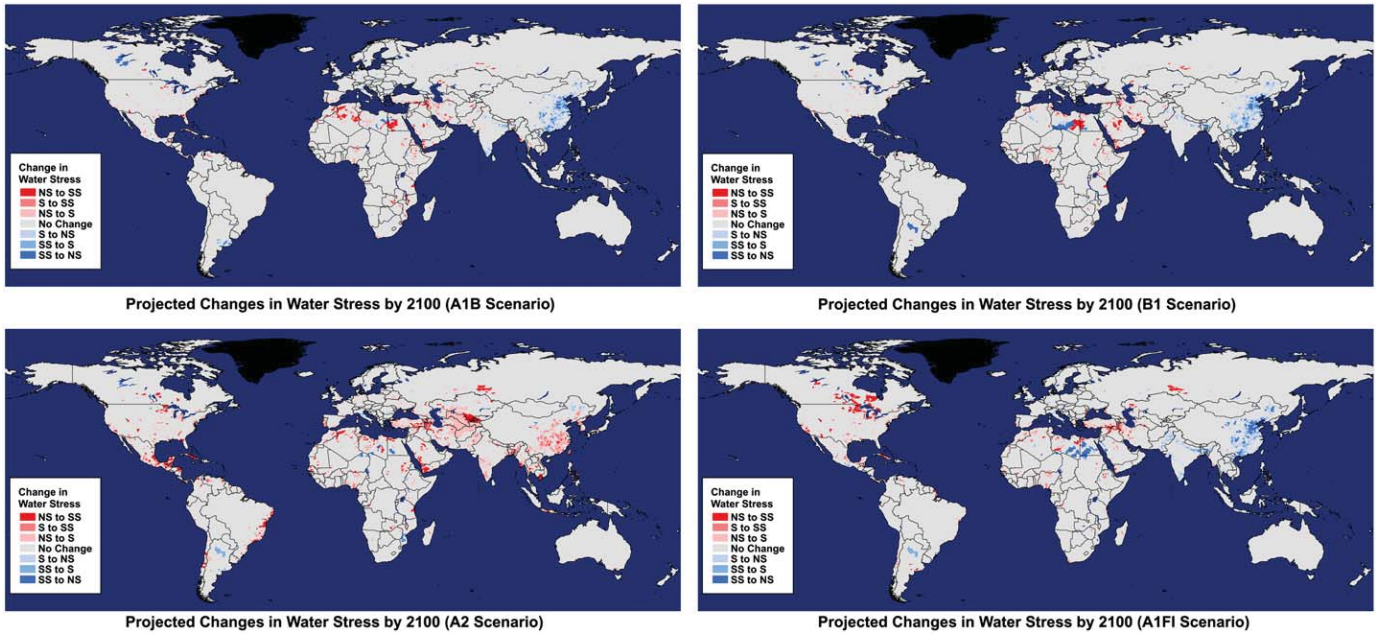

Fig. 6. Projected "Hotspots" of water stress change. Changes in water stress by 2100 are calculated by global watershed under IPCC SRES A1B, B1, A2, and A1F1 scenarios (top to bottom), a range of low to high emission scenarios. Red colors indicate areas of increasing water stress and blue colors indicate areas of decreasing water stress. In eastern Asia, three scenarios (all but the A2 scenario with its associated high population growth) show improvement in eastern Asian conditions. Another notable disagreement among SRES scenarios includes stress conditions in northern Africa; however, because this region has little available water in general, results could be quite sensitive to small variations in projections of P−E. (For interpretation of the references to color in this figure legend, the reader is referred to the web version of this article).

course of the 21st century. Fig. 6 identifies areas that are projected to change stress categories (e.g., stressed to not stressed, not stressed to severely stressed, etc., using definitions from Falkenmark (1986)). In general, this type of visualization could be useful for long term water planning. The most striking potential specific insight can be exemplified in eastern Asia: if population settles at A1/B1 levels and given high A1FI emissions, this region may move from being quite water-stressed to having adequate water supplies in many locales. However, if populations reach A2 levels, then the exact opposite is projected to happen: those same locales are projected to suffer even greater water stresses. Again, this speaks to the recurring potential insight that population change may be a much more critical factor for determining water stress. Based on the *Z*-scores analysis discussed in Section 2.3, caution should be used in interpreting these results, particularly in China, Central America and Central Africa. However, "hotspots" identified through this methodology would seem to warrant future detailed analysis.

4. Conclusions

This study provides a framework for combining climate model and population data into a form that may be useful for water planning. The results presented are intended as exemplary insights that may be obtained via application of the data integration, analysis, and visualization toolkit developed here. The next step may lie in applying this methodology with multiple GCMs, more variations of population projections, and perhaps downstream regional climate and hydrological models as well; this is a critical stage and will allow for a fuller assessment of uncertainty stemming from various quantitative (e.g., physical, structural GCM differences) and qualitative (e.g., expert developed emissions and population change scenarios) sources. Assessing the reliability of individual GCMs and combining them in the context of water availability, perhaps toward developing lower and upper bounds estimates of future water availability, may be important, especially since the simulation of hydrological variables is an acknowledged fundamental gap in climate science (Schiermeier, 2010) with high uncertainty. Steps toward evaluating fuller uncertainty will be crucial for to regional-level policymakers and water resource planners and managers. As discussed in Section 2, this is a complex topic and one we leave to be addressed in future work. In addition, the impact of population and climate driven changes in water quality and how it may affect true net future water availability (e.g., Vörösmarty et al., 2000) has not been discussed here but will be important to address in future work.

We re-emphasize that the region-specific assessments in this paper need to be interpreted as exemplary, first-order scenarios and must be well-caveated in light of uncertainties in population and climate change projections. One contribution of this paper is the design of the problem, especially the approach developed to test the hypothesis concerning relative importance of population versus climate change for water stress. There are two aspects that make this study interesting from the data aspect. First, from the population side, we have used a state-of-the-art high-resolution gridded population dataset, specifically the LandScan data generated at the Oak Ridge National Laboratory, in addition to the IPCC storylines and the CIESIN based regional disaggregation. Second, from the climate model side, we have used the P−E projections from an integrated earth system model, where the disadvantages of lower resolution are assumed in exchange for the opportunity to consider the land-atmosphere feedback effects. In addition, we have developed a toolkit ('toolkit.zip'), which we have provided as an online supplement to this paper to ensure ease of reproducing our results. Future work will need to develop detailed comparisons how regional insights and the scientific hypotheses may differ from previous studies (discussed earlier), which use serially-connected models of global climate, regional climate and hydrology, as well as other datasets or theories for population growth and migration.

Acknowledgments

This research was conducted with funding from the "Understanding Climate Change Impacts: Energy, Carbon, and Water Initiative" within the Laboratory Directed Research and Development (LDRD) Program and the Climate Change Science Institute (CCSI) of the Oak Ridge National Laboratory (ORNL), managed by UT-Battelle, LLC for the U.S. Department of Energy under Contract DEAC05-00OR22725. This work was also supported in part by the National Science Foundation under grant NSF-IIS-1029771. The climate change assessments work performed by ORNL to inform the 2010 Quadrennial Defense Review (QDR) report partially informed the research. The United States Government retains a non-exclusive, paid-up, irrevocable, worldwide license to publish or reproduce the published form of this manuscript, or allow others to do so, for Government purposes.

Appendix A. Supplementary material

Supplementary data associated with this article can be found in the online version at doi:10.1016/j.cageo.2012.01.019.

References

Alcamo, J., Henrichs, T., 2002. Critical regions: a model-based estimation of world water resources sensitive to global changes. Aquatic Sciences 64 (4), 352–362. doi:10.1007/PL00012591.

Alcamo, J., Florke, M., Marker, M., 2007. Future long-term changes in global water resources driven by socio-economic and climatic changes. Hydrological Sciences Journal—Journal Des Sciences Hydrologiques 52 (2), 247–275.

Arnell, N.W., 2004. Climate change and global water resources: SRES emissions and socio-economic scenarios. Global Environmental Change—Human and Policy Dimensions 14 (1), 31–52. doi:10.1016/j.gloenvcha.2003.10.006.

Center for International Earth Science Information Network (CIESIN), 2002. Country-Level Population and Downscaled Projections Based on the B2 Scenario, 1990–2100. Pelisades, NY: CIESIN, Columbia University. Available at 〈http://www.ciesin.columbia.edu/datasets/downscaled〉. (Accessed April 29, 2009).

Development, Concepts and Doctrine Centre (DCDC), 2007. The DCDC Global Strategic Trends Programme 2007–2036. 106 pages, United Kingdom Ministry of Defense.

Deichmann, U., Balk, D., Yetman, G., 2001. Transforming Population Data for Interdisciplinary Usages: From Census to Grid. CIESIN. 〈http://sedac.ciesin.columbia.edu/plue/gpw/GPWdocumentation.pdf〉.

Dobson, J.E., Bright, E.A., Coleman, P.R., Durfee, R.C., Worley, B.A., 2000. LandScan: a global population database for estimating populations at risk. Photogrammetric Engineering and Remote Sensing 66 (7), 849–857.

Drake, J.B., Jones, P.W., Carr Jr., G.R., 2005. Overview of the software design of the community climate system model. International Journal of High Performance Computing Applications 19 (3), 177–186. doi:10.1177/1094342005056094.

Edwards, J., Yang, B., Al-Hmoud, R.B., 2005. Water availability and economic development: signs of the invisible hand? An empirical look at the falkenmark index and macroeconomic development. Natural Resources Journal 45, 953–978.

Falkenmark, M., 1986. Fresh water—time for a modified approach. Ambio 15 (4), 192–200.

Food and Agricultural Organization (FAO), 2003. Review of World Water Resources by Country, edited by A. P. o. F. s. L. a. W. D. Division, United Nations, Rome.

Ganguly, A.R., et al., 2009. Higher trends but larger uncertainty and geographic variability in 21st century temperature and heat waves. Proceedings of the National Academy of Sciences USA 106 (37), 15555–15559.

Greene, A.M., Goddard, L.M., Lall, U., 2006. Probabilistic multimodel regional temperature change projections. Journal of Climate 19, 4326–4343.

International Panel on Climate Change (IPCC), 2007. Summary for Policymakers, Intergovernmental Panel on Climate Change, Fourth Assessment Report.

IPCC, 2000. Special Report on Emissions Scenarios.

Kao, S.-C., Ganguly, A.R., 2011. Intensity, duration, and frequency of precipitation extremes under 21st-century warming scenarios. Journal of Geophysical Research 116 (D16). doi:10.1029/2010JD015529.

Knutti, R., 2010. The end of model democracy? Climatic Change 102 (3–4), 395–404.

Knutti, R., Furrer, R., Tebaldi, C., Cermak, J., Meehl, G.A., 2010. Challenges in combining projections from multiple climate models. Journal of Climate 23 (10), 2739–2758. doi:10.1175/2009JCLI3361.1.

Kodra, E., Steinhaeuser, K., Ganguly, A.R., 2011. Persisting cold extremes under 21st-century warming scenarios. Geophysical Research Letters. doi:10.1029/2011GL047116.

Kundzewicz, Z.W., et al., 2008. The implications of projected climate change for freshwater resources and their management. Hydrological Sciences 53 (1), 3–10.

Le Quéré, C., et al., 2009. Trends in the sources and sinks of carbon dioxide. Nature Geoscience 2 (12), 831–836. doi:10.1038/ngeo689.

Perkins, S.E., Pitman, A.J., Sisson, S.A., 2009. Smaller projected increases in 20-year temperature returns over Australia in skill-selected climate models. Geophysical Research Letters 36, L06710. doi:10.1029/2009GL037293.

Pierce, D.W., Barnett, T.P., Santer, B.D., Gleckler, P.J., 2009. Selecting global climate models for regional climate change studies. Proceedings of the National Academy of Sciences USA 106 (21), 8441–8446.

Raupach, M.R., Marland, G., Ciais, P., Le Quéré, C., Canadell, J.G., Klepper, G., Field, C.B., 2007. Global and regional drivers of accelerating CO_2 emissions. Proceedings of the National Academy of Sciences of the United States of America 104 (24), 10288–10293. doi:10.1073/pnas.0700609104.

Roy, S.B., Limin, C., Girvetz, E., Maurer, E.P., Mills, W.B., Grieb, T.M., 2010. Evaluating Sustainability of Projected Water Demands under Future Climate Change Scenarios Rep. p. 40, Natural Resources Defense Council.

Sabesan, A., Abercrombie, K., Ganguly, A.R., Bhaduri, B., Bright, E.A., Coleman, P.R., 2007. Metrics for the comparative analysis of geospatial datasets with applications to high-resolution grid-based population data. GeoJournal 69 (1–2), 81–91. doi:10.1007/s10708-007-9103-y.

Santer, B.D., et al., 2009. Incorporating model quality information in climate change detection and attribution studies. Proceedings of the National Academy of Sciences USA 106 (35), 14778–14783.

Schiermeier, Q., 2010. The real holes in climate science. Nature 463, 284–287, doi:10.1038/463284a.

Schneider, S.H., Kuntz-Duriseti, K., 2002. Uncertainty and climate change policy. In: Schneider, S.H., Rosencranz, A., Niles, J.O (Eds.), Climate Change Policy: A Survey. Island Press, Washington DC, pp. 53–87. (Chapter 2).

Shiklomanov, I., 1997. Comprehensive Assessment of the Freshwater Resources of the World. World Meteorological Organization, Commission on Sustainable Development.

Smith, R.L., Tebaldi, C., Nychka, D., Mearns, L.O., 2009. Bayesian modeling of uncertainty in ensembles of climate models. Journal of the American Statistical Association 104 (485), 97–116. doi:10.1198/jasa.2009.0007.

Stainforth, D.A., Allen, M.R., Tredger, E.R., Smith, L.A., 2007. Confidence, uncertainty and decision-support relevance in climate predictions. Philosophical Transactions of the Royal Society A 365, 2145–2161.

Tebaldi, C., Means, L.O., Nychka, D., Smith, R.L., 2004. Regional probabilities of precipitation change: a Bayesian analysis of multimodel simulations. Geophysical Research Letters 31, L24213. doi:10.1029/2004GL021276.

Verdin, K.L., Greenlee, S.K., 1996. Development of continental scale digital elevation models and extraction of hydrographic features. In: Proceedings of the Third International Conference/Workshop on Integrating GIS and Environmental Modeling. Santa Fe, New Mexico, January 21–26.

Vörösmarty, C.J., Green, P., Salisbury, J., Lammers, R.B., 2000. Global water resources: vulnerability from climate change and population growth. Science 289 (5477), 284–288. doi:10.1126/science.289.5477.284.

Vörösmarty, C.J., McIntyre, P.B., Gessner, M.O., Dudgeon, D., Prusevich, A., Green, P., Glidden, S., Bunn, E., Sullivan, C.A., Reidy Liermann, C., Davies, P.M., 2010. Global threats to human water security and river biodiversity. Nature 467, 555–561. doi:10.1038/nature09440.

World Research Institute International Water Management Institute, 2003. Water Resources eAtlas. 〈http://multimedia.wri.org/watersheds_2003/index.html〉.